ACS APPLIED MATERIALS & INTERFACES

Research Article

www.acsami.org

Large-Scale Plasmonic nanoCones Array For Spectroscopy Detection

Gobind Das,*[,†,‡] Edmondo Battista,[†,⊥,∥] Gianluigi Manzo,[⊥,#] Filippo Causa,[⊥,∥] Paolo Antonio Netti,[⊥,∥] and Enzo Di Fabrizio[‡]

[‡]PSE division, King Abdullah University of Science and Technology, Thuwal 23955−6900, Saudi Arabia

[⊥]CABHC, IIT @CRIB, Istituto Italiano di Tecnologia, L.go Barsanti e Matteucci 53, 80125 Napoli, Italy

[∥]Interdisciplinary Research Center on Biomaterials (CRIB), University Federico II, P.le Tecchio 80, Napoli, Italy

[#]Department of Applied Science and Technology, Politecnico di Torino, C.so Duca degli Abruzzi 24, 10129 Turin, Italy

Supporting Information

ABSTRACT: Advanced optical materials or interfaces are gaining attention for diagnostic applications. However, the achievement of large device interface as well as facile surface functionalization largely impairs their wide use. The present work is aimed to address different innovative aspects related to the fabrication of large-area 3D plasmonic arrays, their direct and easy functionalization with capture elements, and their spectroscopic verifications through enhanced Raman and enhanced fluorescence techniques. In detail, we have investigated the effect of a Au-based nanoCone array, fabricated by means of direct nanoimprint technique over large area (mm^2), on protein capturing and on the enhancement in optical signal. A selective functionalization of gold surfaces was proposed by using a peptide (AuPi3) previously selected by phage display. In this regard, two different sequences, labeled with fluorescein and biotin, were chemisorbed on metallic surfaces. The presence of Au nanoCones array consents an enhancement in electric field on the apex of cone, enabling the detection of molecules. We have witnessed around 12-fold increase in fluorescence intensity and SERS enhancement factor around 1.75×10^5 with respect to the flat gold surface. Furthermore, a sharp decrease in fluorescence lifetime over nanoCones confirms the increase in radiative emission (i.e., an increase in photonics density at the apex of cones).

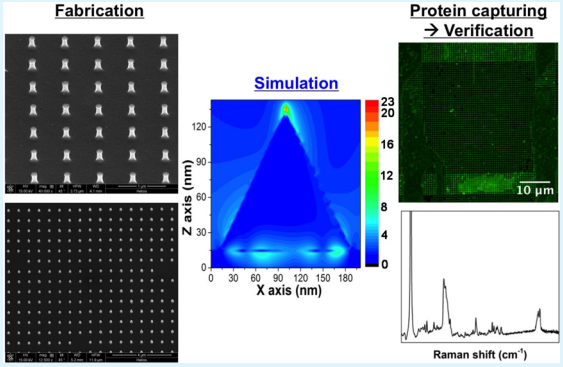

KEYWORDS: *nanocones, surface functionalization, gold binding peptide, fluorescence enhancement, plasmonic device, SERS*

INTRODUCTION

In recent years, an intensive effort has been made to fabricate advanced active or passive optical materials and in particular plasmonic interfaces for a broad range of applications spanning from material engineering to medical science.[1−4] Recent advancement in nanofabrication technology facilitated the design and fabrication of complex structures in a reproducible manner.[5−7] These metal nanostructures allow the confinement and control of light over the nanoscale, associated with the excitation of surface plasmons. Indeed, surface plasmons, collective oscillation of free electrons near a metal surface, can be generated when an electromagnetic radiation is impinged over it. This leads to an accumulation of giant electric field near the metal surface to employ the plasmonic properties for bio/chemical sensors.[8,9] Various plasmonic designs were proposed in the past in realization of miniaturized devices for light manipulation at subwavelength scales. Because of the complex fabrication processes involved in an on-chip device, most studies were limited to the 2D-plasmonic nanofocusing devices[10−14] not enough to achieve the field enhancement for single/few molecules detection. However, there are various research works pointed toward single molecule detection (SMD), where the devices fabricated were prepared using a chemical technique or bottom-up technique, with limited reproducibility.[15−19] 3D plasmonic devices, unlike structures achieved by just metal deposition using top-down method, were fabricated recently by means of electron-beam lithography (EBL) and focused ion beam (FIB) lithography in combination with reactive ion etching (RIE) in order to have a better enhancement and reproducible SERS device for single molecule detection (SMD) or few molecules detection (FMD).[20−23] 3D nanostructure device fabrication could be employed to improve the detection capability of the sensor. The high electric field enhancement shows broad range applications in nonlinear optics,[24] optical rectification,[25] and for single molecule detection.[26] Recently, Chirumamilla et al.[5] realized 3D nanostars structures on Si substrate by employing electron-beam lithography (e-beam lithography) and reactive ion etching (RIE), which allowed us to achieve the enhanced electric field around 50. However, this fabrication process

Received: July 28, 2015
Accepted: September 24, 2015
Published: September 24, 2015

DOI: 10.1021/acsami.5b06887
ACS Appl. Mater. Interfaces 2015, 7, 23597−23604

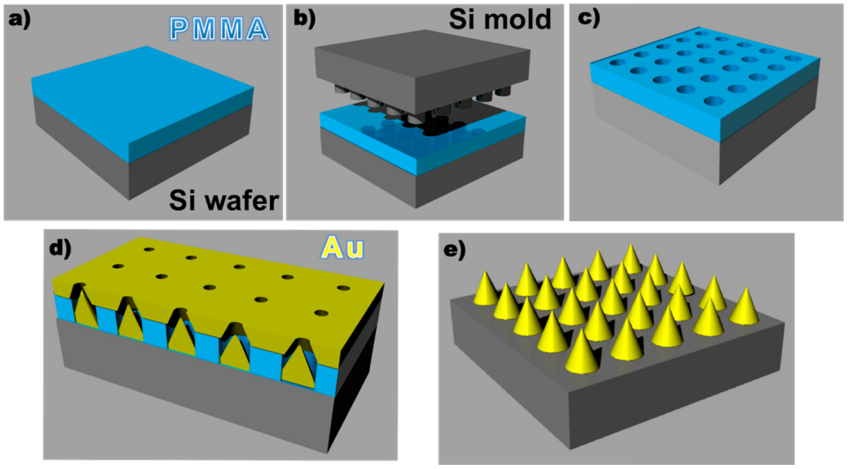

Figure 1. Schematic diagram of fabrication process of large area 3D plasmonic nanoCones array on Si substrate by means of direct nanoimprinting technique. In the scheme, (a) the Si wafer with PMMA resist was (b) imprinted with Si mold, constituting nanoPillars. (c) An array of nanoholes was created. After the Au evaporation over this substrate, the opening of holes reduces as the metal deposition process goes forward. (d) Cross-section of the substrate, thus formed. (e) After the lift-off, 3D nanoCones were achieved. The maximum temperature and maximum pressure employed during this process were 180 °C and 50 bar, respectively.

involves high cost, long production time, and in particular, a small active area, which typically ranges from few to tens of micrometers.[2]

The present work has different innovative aspects: (a) the fabrication of large area 3D plasmonic nanoCone using direct nanoimprinting technique and its plasmonic behavior through finite difference time domain (FDTD) simulation; (b) the direct and easy functionalization of gold-based nanostructures by a selected peptide and their capture ability of large molecules based on the high affinity pair biotin/Streptavidin; (c) the spectroscopic verifications of adsorbed molecules through enhanced Raman and enhanced fluorescence techniques.

Many researchers were involved in the fabrication of nanostructures using nanoimprint lithography (NIL) technique since its introduction in 1995 by Chou et al.[27] This technique facilitates the fabrication of nanostructures with the spatial resolution down to sub 10 nm, keeping the fabrication cost and production time significantly low. Various nanostructures, fabricated using this technique, and following UV curing of polymers, were reported with limited application of the device.[28−30] Very few reports can be found which are related to the 3D nanostructured devices, fabricated by direct NIL technique[31,32] and their spectroscopic properties. In this work, various shapes (nanoCones, nanoSpinningTop, nanoBowl) and size of 3D plasmonic nanostructures in a large surface area were achieved by altering the NIL process by combination with metal evaporation in different regimes. In this work, we focused our attention especially on large nanoCones substrates as these structures provide an effective confinement of electric field at the apex of cone.[20] However, further study, herein, shows the multifacet properties of this structure for protein capturing and bio/material analysis through Raman and fluorescence spectroscopy. Systematic and in-detailed analyses were performed to investigate for various applications.

The 3D nanoCones array substrates were thereafter employed for sensing applications. In this regard some concerns, related to the functionalization of metal nanostructures, were taken into consideration in order to provide a suitable surface chemistry thus allowing to bind the specific capture molecules, such as antibody, DNA or peptides.[33] The most common strategy to selective functionalization of gold is represented by mixed self-assembled monolayers of alkanethiolates.[34] Even though lots of efforts have been spent on this technology as the high cost of the building blocks and the complex procedures limit its use in tailoring the chemistry of the inorganic surfaces. However, **g**enetically **e**ngineered **p**eptides for **i**norganics (GEPI), short peptides with high affinity for inorganic surfaces, have already been demonstrated to be an attractive alternative in a wide range of applications in terms of costs and simplicity of procedures.[35,36] Indeed, GEPIs can bind the surfaces simply by chemisorption, usually from aqueous solutions. Phage Display, a combinatorial high throughput screening technique, is capable to select short peptide sequences for inorganics with high affinity.[37] Our group have already selected a gold binding peptide (AuPi3) and characterized its affinity toward gold by using Phage Display.[36] Here, exploiting the affinity of AuPi3 toward gold, we demonstrate the one pot introduction of a capture element on the 3D nanostructures simply by chemisorption. In this regard, AuPi3 is modified at the C-terminus flanking region with another peptide of 10 amino-acids and the affinity toward gold and, therefore, the ability to capture a protein (Streptavidin) were investigated by both techniques: fluorescence emission imaging and Raman spectroscopy.

Fluorescence-based imaging is very much popular in the biological field. An increase in fluorescence intensity and stability of fluorophores is required to increase the sensitivity and detection limit of new integrated array systems.[38] Periodic silver-based substrates were discussed for enhanced fluorescence spectroscopy.[39] The report suggests that the intensity of fluorescein molecules could be enhanced when is adsorbed on Ag square nanostructure. The plasmonic enhancement can be further increased if we use 3D nanostructures, especially cone structure.[5,20,40] In this work, 3D plasmonic nanostructures were employed to probe the molecule of interest using spectroscopic techniques (fluorescence and Raman) . In this regards, two different assay formats (primary and secondary fluorescent molecules) were examined. To shed light on the mechanism of fluorescence enhancement due to the gold nanostructures, fluorescence lifetime imaging microscopy (FLIM) coupled with multiphoton laser source proved effective in probing the microenvironment of fluorescent molecules and the metal

DOI: 10.1021/acsami.5b06887
ACS Appl. Mater. Interfaces 2015, 7, 23597−23604

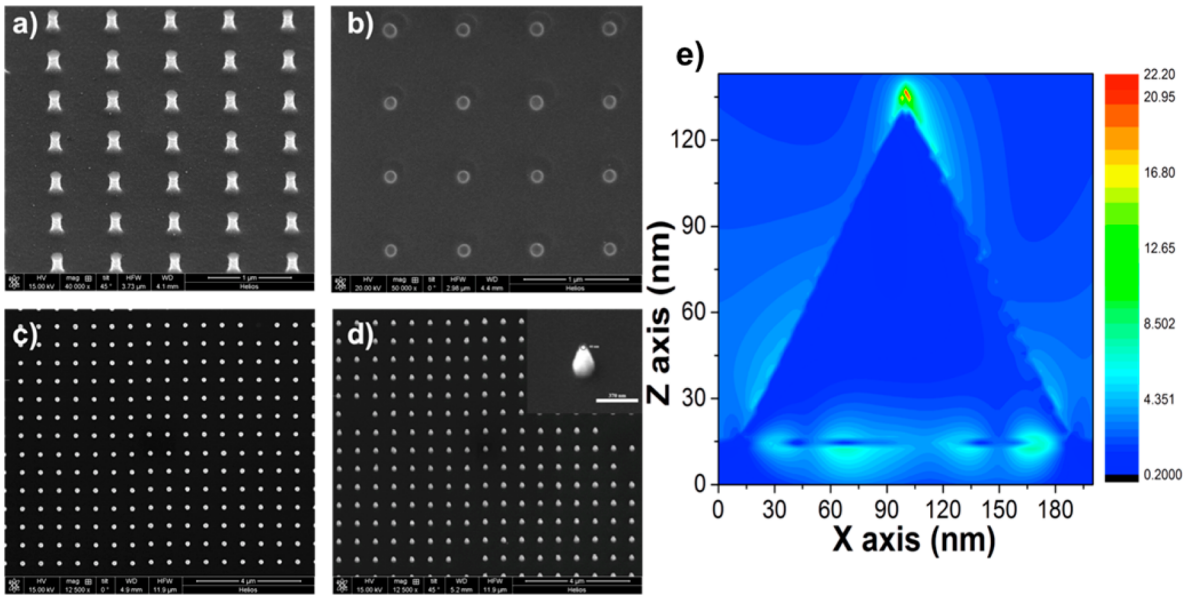

Figure 2. SEM images of (a) Si nanoimprinter mold at tilt angle 45°, (b) array of nanoholes after imprinting, (c) top-view of gold nanoCone array, and (d) array of nanoCone structures at tilt angle of 45°. In the inset of d, a zoomed image of nanoCone is also illustrated. The radius of curvature of nanoCone is 22 nm. The nanostructures were fabricated in the large area 750 mm × 1000 mm. (e) The electric field distribution is calculated for the nanoCone (h, 110 nm; base diameter, 180 nm) fabricated over Si substrate.

enhanced fluorescence effect. In addition, surface-enhanced Raman scattering (SERS) effect is also investigated on these substrates. The 3D plasmonic nanostructures with fluorophores were examined in this regard and was found that the enhancement in Raman signal could reach in the range of 1×10^5 to 1×10^6, which enables the detection of analyte with the concentration down to femtomolar[41,42] and even single molecule detection.[5,43]

The novelty of this work is to use gold-based 3D nanoCone plasmonic structures, over large area (fabricated by means of direct NIL technique), for selective functionalization by peptides to carry out the specific protein capture and, thereafter, to analyze the substance by means of fluorescence and Raman technique.

EXPERIMENTAL SECTION

Fabrication Process. Obducat Nano Imprint Lithography system was employed for fabrication of 3D- plasmonic device. PMMA (A8, 1:2) was spin-coated with 4000 rpm (thickness: around 250 nm) onto Si wafer. The mold was fabricated by means of combining EBL and RIE. The mold consists of an array of nanoPillars with diameter, height and the gap between two nanoCones of around 185, 250, and 520 nm, respectively. The mold was silanized using an organic molecule, Trichloro (1H,1H,2H,2H-perfluorooctyl) silane, to facilitate the easy detachment of mold from the resist. Direct imprinting was performed on PMMA coated Si substrate. To ensure that lift-off could function in a proper manner and a patterned substrate could be achieved, the sample was exposed to O_2 plasma (70 W, 200 s, 50% O_2 and bias: 270 V) to clean the residual photoresist within the holes. A layer of Ti/Au (5 nm/110 nm) was evaporated over the surface with a deposition rate of 0.5−2.0 Å/s to achieve the desired nanostructures. Titanium layer is deposited as an adhesion layer. After metal deposition, the residual PMMA was lifted off leaving gold nanostructures on Si substrate. The opening area of the hole reduces as the deposition process goes on and thus forming different nanostructure in the hole. The lift-off process results the substrate with an array of gold nanoCones with the base diameter, height and intercone distance of around 180, 110, and 520 nm, respectively. The schematic fabrication process in detail is shown in Figure 1a−e. The rate of deposition must be kept above 1.5 Å/s in order to attain the conical structures or else it will turn out the different structures (see Supporting Information, section 1).

FDTD Simulation on nanoCones. To provide the theoretical confirmation of the plasmonic behavior of this design, finite difference time domain (FDTD) simulation was carried out for nanoCone structure by means of the Lumerical, FDTD solution (Lumerical Solutions Inc. FDTD Solutions version 8.0.1. http://www.lumerical.com/tcad-products/fdtd/), a commercial software package. The gold cone (h = 110 nm and base diameter of 180 nm) is designed over Si substrate. The perfectly matched layer (PML) is created around the cone to avoid any simulation problem with open boundary design. In order to resolve the focusing spot at any point of the structure, the subgriding method is employed to achieve the mesh size down to $2 \times 2 \times 2$ nm^3. The analysis was performed by considering the "Johnson and Christy" dispersion curve for Au material whereas "Palik" dispersion for Si.[44,45]

Surface Functionalization. The device surface was treated by GBPs (gold binding peptides), with a common sequence previously selected by phage display to be selective for gold (AuPi3: TLLVIRGLPGAC).[36] GBP (AuPi3-G_4-RGD, MW 1953.26 Da), GBP-FITC (AuPi3-G_4-RGDSPK(FITC), MW: 2469.82 Da) and GBP-Biotin (AuPi3-G_4-RGDSPK(Biotin), MW: 2307.73 Da) (purchased from Proteogenix, France) were dissolved in HBS (10 mM Hepes, 150 mM NaCl, 3 mM EDTA, pH 7.4). The stock solutions at the concentration of 256 μM, 216 μM and 30 μM were prepared for GBP and GBP-Biotin and GBP-FITC, respectively. A solution of Atto425-Streptavidin (MW: 61200 Da) (purchased by Sigma-Aldrich) was prepared in HBS solvent at the concentration of 16 μM. Gold surface was cleaned in a 5% (w/v) water solution of sodium hypochlorite for 5 min, then washed with ethanol (95%) and dried with nitrogen. The molecular binding was carried out by dropping 2 μL of solution on gold surfaces. The drop was left to adsorb for 30 min, rinsed with 3 mL HBS afterward, and then dried with nitrogen.

Electron Microscopy Characterization. A scanning electron microscope (SEM) was used to observe the morphologies of the nanoCone-based devices by means of FEI instrument (dual beam). The morphology of Si nanoPillars (used as mold), the nanohole (formed after the imprinting process), and the nanoCones (attained after the metal deposition followed by lift-off process in acetone solution) from top and tilted at 45° are shown in Figure 2a−d. In the

DOI: 10.1021/acsami.5b06887
ACS Appl. Mater. Interfaces 2015, 7, 23597−23604

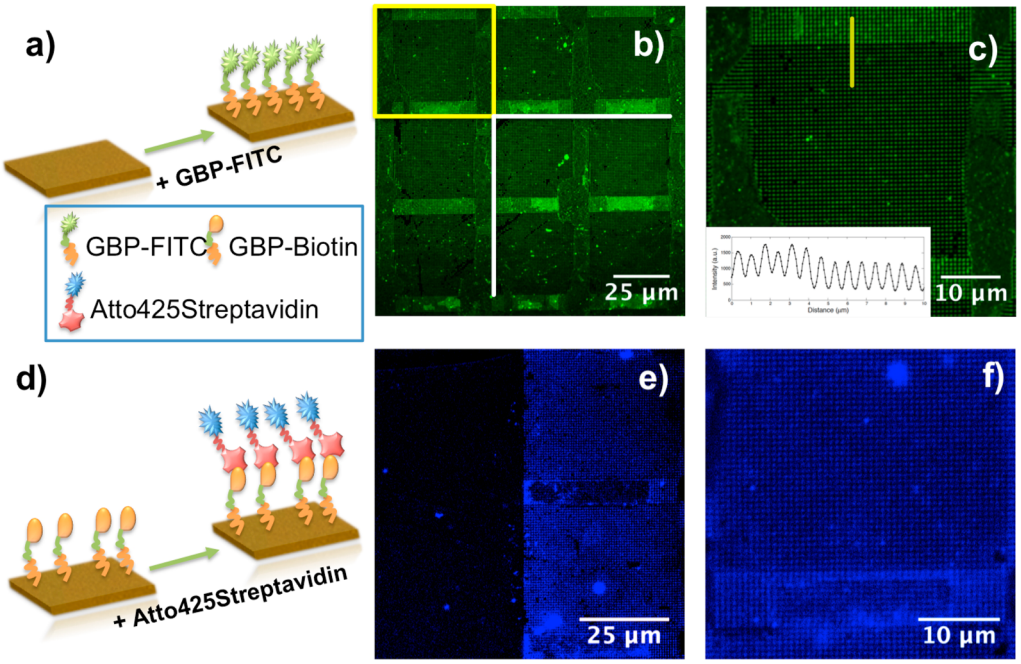

Figure 3. (a) Adsorption of GBP-FITC on gold surface is shown. (b, c)Fluorescence images of GBP-FITC chemisorbed to the device with different magnifications. In the inset, the fluorescence intensity profile is shown. (d) capture of the ATTO425-Streptavidin by the device functionalized with GBP-Biotin; (e, f) fluorescence images of the captured ATTO 425-Streptavidin with different magnifications.

inset of Figure 2d, the zoomed image of nanoCone with radius of curvature (RoC) around 22 nm can be clearly observed.

Fluorescence Microscopy. Confocal fluorescence and lifetime images (FLIM) were recorded by means of a Leica inverted microscope SP5 from Leica Microsystems using a water immersion objective 25x (NA: 0.95). To investigate the binding of GBP-FITC, we excited the system with an Ar^+ laser at 488 nm and the emission bandwidth was from 520 to 600 nm, whereas for GBP-Biotin and Atto425-Streptavidin binding assays, the molecules were excited with an Ar^+ laser at 458 nm and the emission bandwidth was fixed in the range of 500−550 nm. All the images were collected at 12 bit color depth with a resolution of 1024 × 1024 pixels.

Fluorescence lifetime images (FLIM) of GBP-FITC adsorbing nanostructures were acquired by using a pulsed Multiphoton Laser source (120 fs, 80 MHz, Ultra, Chamaleon, Coherent, Santa Clara CA, US) implemented in the time-domain using a time-correlated single photon counting (TCSPC) module. The laser was tuned to 780 nm for two-photon excitation of fluorescein derivative by TCSPC, operating the laser at excitation 800 nm. Images and lifetime data were analyzed by using SymPhoTime software (PicoQuant, Germany).

Quartz Crystal Microbalance Measurements. The adsorption measurements over gold-coated surface were performed by means of KSV QCM-Z 500. The sensor crystals were composed of AT-cut quartz layered with thermally evaporated gold and had a resonant frequency of 5 MHz. The results were showed at third overtone of the fundamental frequency with a resolution time of less than 1 s. The crystal was cleaned using an alkaline oxidative treatment and then washed in ethanol and acetone for three times. HBS buffer was first loaded into the liquid cell, then, when baseline signal was stable, GBP solutions were added. Before further injections, cell was rinsed twice with HBS.

Surface-Enhanced Raman Scattering. SERS measurements were performed by means of DXR Raman microscope (Thermo Fischer Scientific) with spectral resolution around 1 cm^{-1} with the help of 1800 grooves/mm. The molecules were excited with 780 nm laser wavelength in backscattering configuration through a 100× objective (NA: 0.90). The scattering was collected in the whole range of 200−2500 cm^{-1}, keeping the laser power 5 mW (in case of a patterned surface). The spectra were analyzed using Omnic software (in-built).

RESULTS AND DISCUSSIONS

The large area 3D-plasmonic substrates (750 × 1000 μm^2) with an array of nanoCones were fabricated by means of direct nanoimprint lithography technique.[46] The nanostructures with different shapes were fabricated by selecting the adequate metal deposition rate and thickness (see the Supporting Information, section 1). This ascertains the fabrication process versatile, cost and time effectiveness to fabricate the 3D-plasmonic substrate in large active area. Plasmonic behavior was tested by means of FDTD (finite difference time domain) simulation using commercial software, Lumerical solutions using linearly polarized light (as in experimental setup). In the past, few numerical calculations were performed and found that the best experimental configuration to achieve the maximum plasmonic effect is to illuminate the nanostructures by radially polarized light source.[28,47] The gold nanostructures (nanoCones array) over Si substrates were modeled with structural geometry such as base and height of the cone are fixed to 180 and 110 nm, respectively. The electric field distribution for the nanoCone structure was calculated for 760 nm, shown in Figure 2e. The simulation findings show the confinement of an electric field over the apex of the cone in accordance with the report in the past.[28,48] In this case, the confined electric field at the apex of the cone is around 20 with respect to the incident. The result, therefore, suggests that the molecules residing close to the apex will contribute the maximum enhancement with respect to the base of the nanostructure. In terms of Raman signal enhancement, the optical signal would be almost 2.4 × 10^5 with respect to what is observed at the base of cone. Such surfaces were functionalized by simple chemisorption of a specific peptide selective for gold. As previously demonstrated by Causa et al.,[36] the AuPi3 sequence, selected by phage display, can bind selectively with higher affinity gold surfaces. In

DOI: 10.1021/acsami.5b06887
ACS Appl. Mater. Interfaces 2015, 7, 23597−23604

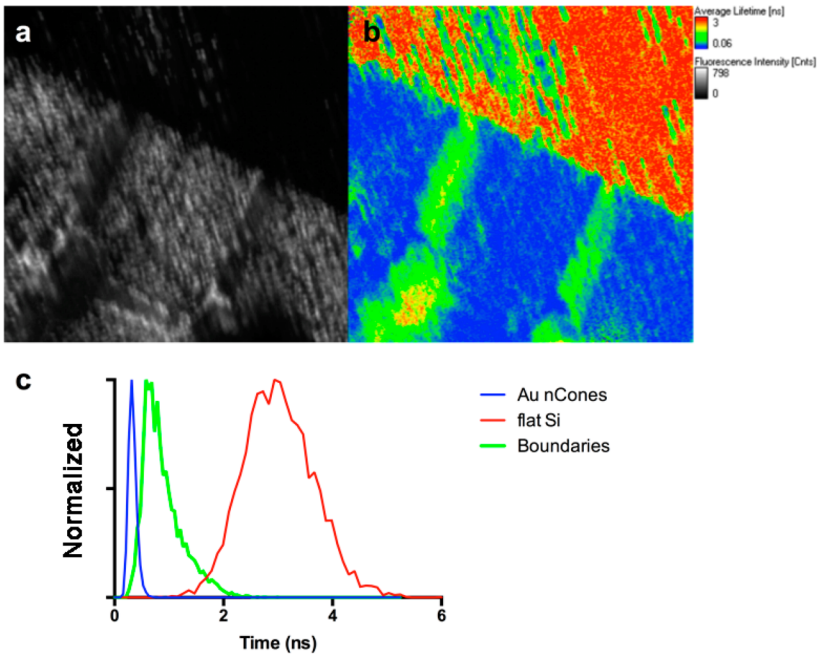

Figure 4. (a) Fluorescence intensity image and (b) fluorescence lifetime image of Au nanoCones device in the presence of 30 μM GBP-FITC solution. In c) are the histograms of average lifetimes taken over different regions of the nanostructured device (blue, Au-nanoCones; green, boundary regions between the square of isolated Au-nanoCones; red, continuous flat Si). Image size is 100 μm × 100 μm. Two-photon excitation laser (780 nm) power 3 W, emission range 500−530 nm.

this work, we modified the sequence of the original peptide in order to accommodate another peptide sequence of 10 amino acids at the C-terminus, mimicking a capture element for large molecule. In this work, we employed biotin to demonstrate the capturing of Streptavidin. The adsorption of two different peptides, GBP-FITC (a Fluorescein derived peptide) and GBP-Biotin (a biotin-derived peptide able to capturing Atto425-Streptavidin) was verified on the device. The flowchart of the adsorption process of GBP-FITC on gold is shown in Figure 3a and the confocal fluorescence image of GBP-FITC molecules (conc.: 30 μM), adsorbed on nanoCones is exhibited in Figure 3b. The zoomed image of squared area is shown in Figure 3c in which all the nanoCones with a base diameter around 180 nm are perfectly visible and resolved with each other. The intensity profile of fluorescence image is also depicted in the inset, which shows that even the smaller base area of nanoCone (in the range of 180 nm) can be easily resolved without any additional experimental modification. The fluorescent GBP-FITC, herein, at different concentrations (0.3−30 μM) was examined over the substrates (see the Supporting Information, section 2). The comparative fluorescence images (on the patterned surface and on gold evaporated flat quartz surface) with intensity profile were also illustrated. It clearly reveals that though the number of molecules at the apex of nanoCone surface is lesser than on flat surface, the fluorescence intensity increases up to around 12-fold with respect to the flat gold surface, showing a strong fluorescence enhancement due to electric field localization on the apex of Cone (see the Supporting Information, section 2).

Indeed, this effect is also evidenced by lifetime imaging of GBP-FITC solutions in direct contact with nanostructures (see Figure 4). As can be seen the fluorescent molecules experience different fluorescence decay pattern: on silicon surface with a broad distribution of lifetimes in the range of 2.20−3.78 ns; on the Au nanoCones a narrow distribution around 0.32 ns; while at boundaries between the square isolated nanoCones (where inter nanoCones distance is 500 nm) a broader range of lifetimes between 0.48 and 1.21 ns. The decreased lifetime near the isolated nanoCones account also for high fluorescence intensity that can be ascribable to the coupling effect at metal surface. As already described by Lakowicz and Geddes,[49,50] metal enhanced fluorescence (MEF) occurs when fluorophores are positioned in the near-field, typically less than 5 nm from a metal and is characterized by an increased fluorescence intensity and a decreased fluorescence lifetime. As reported, MEF is also correlated to an enhanced fluorophore photostability as the fluorophores spend less time "'on average"', in an excited state, prior to their return to the ground state, and are subsequently less prone to photodestruction.

Furthermore, biotin labeled peptide-specific adsorption was also carried out in order to demonstrate the one-pot functionalization and also the secondary binding is very much localized over this device. Prior to this experiment, various measurements were performed by means of QCM technique in order to demonstrate that the adsorption of Atto-Streptavidin molecule on Au surface does not occur if the metal surface is not initially adsorbed with GBP-Biotin molecule (see Supporting Information, section 3). With this confirmation, biotinylated AuPi3 peptide (MW > 60 kDa) was used as a capturing system over the Au-based nanoCone surface and, thereafter, Streptavidin labeled with Atto425 (a fluorescent dye molecule) was immobilized on the nanostructure. The use of biotinylated AuPi3 peptide can explain why the nonradiative lifetime -the quenching- does not kill the fluorescence. In fact, the nonradiative to radiative decay goes like $1/d^3$ where, d is the distance of the molecule fluorophore from the metal. In case of direct absorption of the fluorophore, the first layer of molecules (those in contact with the gold tip) is quenched and a second layer will be enhanced. The confocal fluorescence imaging was recorded in order to localize the fluorescent Streptavidin molecule, attached to the biotinylated peptide surface. Indeed,

DOI: 10.1021/acsami.5b06887
ACS Appl. Mater. Interfaces 2015, 7, 23597−23604

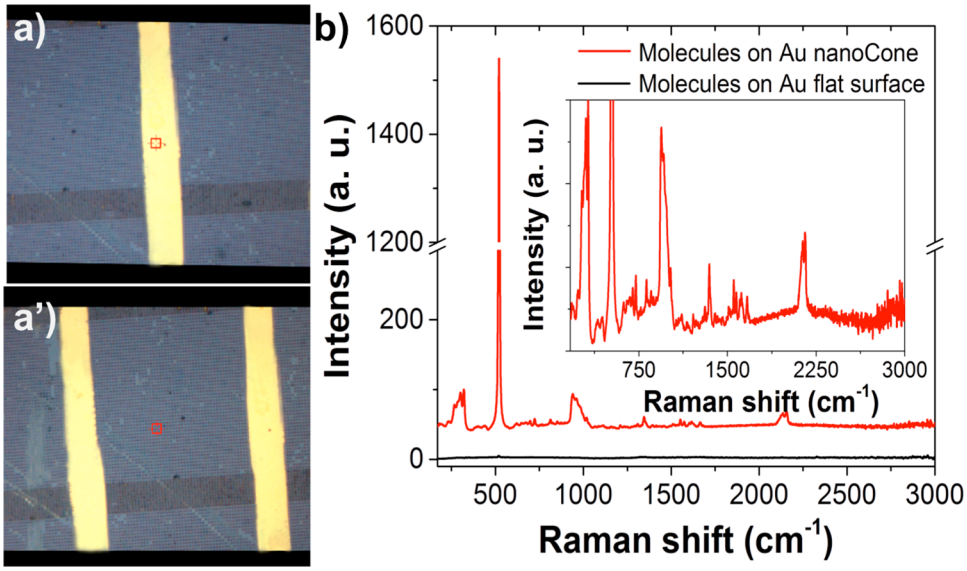

Figure 5. (a, a′) Optical images of unpatterned and patterned surface where the SERS measurements were performed. (b) SERS spectra at unpatterned surface (black line) and at nanoarray patterned area. Zoomed SERS spectrum in the spectral range of 980−2250 cm^{-1} is also shown in the inset. In the case of flat gold surface, the integration time and power both were kept 5× times higher with respect to the SERS measurements (patterned surface) in order to achieve some signal from the molecules deposited over it.

the selectivity and affinity of AuPi3 is preserved even after the derivatization of the flaking region of gold binding domain. The schematic diagram of the whole adsorption process and the confocal fluorescence images of Streptavidin are shown in Figure 3d−f). The adsorption of biotin−streptavidin (two-step processes) over Au nanoCone shows the compatibility of these biomolecular activities on this device again. The enhancement in fluorescence intensity could be due to the increase in radiative decay rate, especially due to resonance energy transfer in the presence of metal nanostructures causing an enhancement in localized electric field in proximity of metal surface mainly due to "antenna effect".[51] To support this behavior, we performed lifetime fluorescence imaging on the GBP-FITC coated nanostructures, shown in Figure 4. Figure 4a shows the fluorescence intensity of the device; the maximum fluorescence intensity is observed where the nanoCones are present. The confirmation of increase in radiative emission is clearly observed from lifetime fluorescence imaging: the fluorophore lifetime decreases sharply for the nanoCones structures due to the increase in photonic density.[52]

In addition, the present device with nanoCone plasmonic structures[20] shows an interesting behavior of exhibiting an enhancement for Raman scattering too. The most dominating factor in the case of SERS is localized electric field on the metal surface. With the radius of curvature 22 nm of Au nanoCone, high electric field on the apex of a cone can be confined to detect low concentrated molecules. Confocal Raman scattering measurements were performed using 780 nm on periodic array of nanoCone pattern and on flat gold surface. Optical images of laser focusing on unpatterned and patterned area are shown in Figure 5a, a′, respectively. SERS spectra of FITC molecule deposited over patterned and flat Au surface are shown in Figure 5b. The sharp band, centered at 520 cm^{-1}, and the broad bands around 320 and 950 cm^{-1} are related to the Si wafer underneath the nanoCones. Various vibrational bands in the range of 980−2300 cm^{-1} can be associated with the characteristic bands of Fluorescein molecule.[53] Small sharp band at 1018 cm^{-1} can be related to the ring stretching. Various intense bands centered at 1345, 1507, and 1664 cm^{-1} were related to the xanthene ring stretching of C−C vibrations. Other vibrational bands, centered at 1553, 1573, and 1616 cm^{-1}, can be associated with the C−H bending (aromatic), C═O stretching and combination of ring stretching and bending of CO-H, respectively. The broad band around 2100 cm^{-1} is related to − S-CH_3 which is from the peptide attached to the Au surface. The black spectrum is collected from the same molecules attached on the flat surface, which show a spectrum without any Raman significance. SERS enhancement factor for these nanoCones based device with respect to the flat Au surface is estimated to be around 1.75 × 10^5. The calculation of SERS enhancement can be found in detail in Supporting Information, section 4.

CONCLUSIONS

Large- area Au-based nanostructures 3D-plasmonics devices of different shape (nanoCone, nano SpinningTop, nanoBowls, nanoGlasses, etc.) were fabricated by means of direct nanoimprinting technique, showing versatile and straightforward in terms of device design. The nanoCone device (h = 110 nm, base diameter = 180 nm, Apex radius of curvature = 22 nm, intercone distance = around 500 nm) was employed in order to investigate the adsorption of molecules. In this regards, two molecules such as Fluorescein and Biotin−Streptavidin (direct adsorption and two-step adsorptions) were examined for adsorption over array of Au-nanoCones. Confocal fluorescence imaging shows successful adsorption of both molecules with well-resolved nanoCones of around 180 nm base diameter. The fluorescence intensity profile shows an enhanced molecular fluorescence (up to around 12-fold) due to the electric field localization on the apex of Cone. Furthermore, lifetime imaging and SERS measurements performed for GBP-FITC, deposited over this device, evidenced a remarkable enhancement for both the spectroscopic techniques. For this device the SERS enhancement factor is estimated to be around 1.75 × 10^5 with respect to the flat Au surface. These findings show a remarkable significance of this device for enhanced Raman and

DOI: 10.1021/acsami.5b06887
ACS Appl. Mater. Interfaces 2015, 7, 23597−23604

fluorescence spectroscopy. The easy, flexible, cost and time effectiveness required for 3D-plasmonic device fabrication would also make these substrates to be used for bio/chemical-analysis, opening the way to their large-scale applications. In addition, the present device could be employed as a disposal multiplex nanoarray for bioactivities. Further research is needed to improve the optical behavior by optimizing the height and the distance between two nanoCone.

■ ASSOCIATED CONTENT

Supporting Information

The Supporting Information is available free of charge on the ACS Publications website at DOI: 10.1021/acsami.5b06887.

Device fabrication; confocal fluorescence spectroscopy comparison; quartz crystal microbalance (QCM) measurements; calculation of SERS enhancement factor (PDF)

■ AUTHOR INFORMATION

Corresponding Author

*E-mail: gobind.das@kaust.edu.sa.

Author Contributions

†G.D. and E.B. contributed equally. G.D. conceived the idea, realized the gold nanostructures, performed the Raman characterization and the numerical calculations; supervised the experimental part of the work and wrote the manuscript. E.B. conceived the idea, designed the experimental plan, performed the functionalization with gold peptides and the fluorescence characterization, and wrote the manuscript. G.M. performed the fluorescence and QCM characterization and helped in writing the manuscript. F.C., P.A.N., and E.D.F. discussed the results and commented on the manuscript. The manuscript was written through contributions of all authors. All authors have given approval to the final version of the manuscript.

Notes

The authors declare no competing financial interest.

■ ACKNOWLEDGMENTS

The authors are grateful to Dr Fabio Formiggini for his help in lifetime measurements and comment of the results. This work was supported by project ITEM (*Infrastruttura per Tecnologie BioMEMS di Sensing Avanzato per Monitoraggio e Diagnostica Ambientale e Alimentare)* PONa3_00077 founded by UE, MIUR and Ministero dello Sviluppo Economico. G.D. acknowledges Chirumamilla M. with help for EBL writing.

■ REFERENCES

(1) Zhang, B.; Kumar, R. B.; Dai, H.; Feldman, B. J. A Plasmonic Chip for Biomarker Discovery and Diagnosis of Type 1 Diabetes. *Nat. Med.* **2014**, *20* (8), 948−53.

(2) Vo-Dinh, T.; Fales, A. M.; Griffin, G. D.; Khoury, C. G.; Liu, Y.; Ngo, H.; Norton, S. J.; Register, J. K.; Wang, H. N.; Yuan, H. Plasmonic Nanoprobes: From Chemical Sensing to Medical Diagnostics and Therapy. *Nanoscale* **2013**, *5* (21), 10127−40.

(3) Boriskina, S. V.; Ghasemi, H.; Chen, G. Plasmonic Materials for Energy: From Physics to Applications. *Mater. Today* **2013**, *16* (10), 375−386.

(4) Manikas, A. C.; Aliberti, A.; Causa, F.; Battista, E.; Netti, P. A. Thermoresponsive Pnipaam Hydrogel Scaffolds with Encapsulated Aunps Show High Analyte-Trapping Ability and Tailored Plasmonic Properties for High Sensing Efficiency. *J. Mater. Chem. B* **2015**, *3* (1), 53−58.

(5) Chirumamilla, M.; Toma, A.; Gopalakrishnan, A.; Das, G.; Zaccaria, R. P.; Krahne, R.; Rondanina, E.; Leoncini, M.; Liberale, C.; De Angelis, F.; Di Fabrizio, E. 3d Nanostar Dimers with a Sub-10-Nm Gap for Single-/Few-Molecule Surface-Enhanced Raman Scattering. *Adv. Mater.* **2014**, *26* (15), 2353−8.

(6) Lassiter, J. B.; Sobhani, H.; Fan, J. A.; Kundu, J.; Capasso, F.; Nordlander, P.; Halas, N. J. Fano Resonances in Plasmonic Nanoclusters: Geometrical and Chemical Tunability. *Nano Lett.* **2010**, *10* (8), 3184−9.

(7) Nagpal, P.; Lindquist, N. C.; Oh, S. H.; Norris, D. J. Ultrasmooth Patterned Metals for Plasmonics and Metamaterials. *Science* **2009**, *325* (5940), 594−7.

(8) Brolo, A. G. Plasmonics for Future Biosensors. *Nat. Photonics* **2012**, *6* (11), 709−713.

(9) Stockman, M. I. Nanoplasmonics: Past, Present, and Glimpse into Future. *Opt. Express* **2011**, *19* (22), 22029−22106.

(10) Das, G.; Chirumamilla, M.; Toma, A.; Gopalakrishnan, A.; Zaccaria, R. P.; Alabastri, A.; Leoncini, M.; Di Fabrizio, E. Plasmon Based Biosensor for Distinguishing Different Peptides Mutation States. *Sci. Rep.* **2013**, *3*, 1792.

(11) Shegai, T.; Chen, S.; Miljkovic, V. D.; Zengin, G.; Johansson, P.; Kall, M. A Bimetallic Nanoantenna for Directional Colour Routing. *Nat. Commun.* **2011**, *2*, 481.

(12) Das, G.; Chirumamilla, M.; Gopalakrishnan, A.; Toma, A.; Panaro, S.; Proietti Zaccaria, R.; De Angelis, F.; Di Fabrizio, E. Plasmonic Nanostars for Sers Application. *Microelectron. Eng.* **2013**, *111*, 247−250.

(13) Desiatov, B.; Goykhman, I.; Levy, U. Plasmonic Nanofocusing of Light in an Integrated Silicon Photonics Platform. *Opt. Express* **2011**, *19* (14), 13150−13157.

(14) Genet, C.; Ebbesen, T. W. Light in Tiny Holes. *Nature* **2007**, *445* (7123), 39−46.

(15) Le Ru, E. C.; Blackie, E.; Meyer, M.; Etchegoin, P. G. Surface Enhanced Raman Scattering Enhancement Factors: A Comprehensive Study. *J. Phys. Chem. C* **2007**, *111*, 13794−13803.

(16) Xu, H.; Bjerneld, E. J.; Kall, M.; Borjesson, L. Spectroscopy of Single Hemoglobin Molecules by Surface Enhanced Raman Scattering. *Phys. Rev. Lett.* **1999**, *83* (21), 4357−4360.

(17) Lim, D. K.; Jeon, K. S.; Hwang, J. H.; Kim, H.; Kwon, S.; Suh, Y. D.; Nam, J. M. Highly Uniform and Reproducible Surface-Enhanced Raman Scattering from DNA-Tailorable Nanoparticles with 1-Nm Interior Gap. *Nat. Nanotechnol.* **2011**, *6* (7), 452−60.

(18) Li, J. F.; Huang, Y. F.; Ding, Y.; Yang, Z. L.; Li, S. B.; Zhou, X. S.; Fan, F. R.; Zhang, W.; Zhou, Z. Y.; Wu de, Y.; Ren, B.; Wang, Z. L.; Tian, Z. Q. Shell-Isolated Nanoparticle-Enhanced Raman Spectroscopy. *Nature* **2010**, *464* (7287), 392−5.

(19) Sawai, Y.; Takimoto, B.; Nabika, H.; Ajito, K.; Murakoshi, K. Observation of a Small Number of Molecules at a Metal Nanogap Arrayed on a Solid Surface Using Surface-Enhanced Raman Scattering. *J. Am. Chem. Soc.* **2007**, *129*, 1658−1662.

(20) De Angelis, F.; Das, G.; Candeloro, P.; Patrini, M.; Galli, M.; Bek, A.; Lazzarino, M.; Maksymov, I.; Liberale, C.; Andreani, L. C.; Di Fabrizio, E. Nanoscale Chemical Mapping Using Three-Dimensional Adiabatic Compression of Surface Plasmon Polaritons. *Nat. Nanotechnol.* **2010**, *5* (1), 67−72.

(21) Scholder, O.; Jefimovs, K.; Shorubalko, I.; Hafner, C.; Sennhauser, U.; Bona, G. L. Helium Focused Ion Beam Fabricated Plasmonic Antennas with Sub-5 Nm Gaps. *Nanotechnology* **2013**, *24* (39), 395301.

(22) Genevet, P.; Tetienne, J. P.; Gatzogiannis, E.; Blanchard, R.; Kats, M. A.; Scully, M. O.; Capasso, F. Large Enhancement of Nonlinear Optical Phenomena by Plasmonic Nanocavity Gratings. *Nano Lett.* **2010**, *10* (12), 4880−3.

(23) De Angelis, F.; Liberale, C.; Coluccio, M. L.; Cojoc, G.; Di Fabrizio, E. Emerging Fabrication Techniques for 3d Nano-Structuring in Plasmonics and Single Molecule Studies. *Nanoscale* **2011**, *3* (7), 2689−2696.

(24) De Angelis, F.; Malerba, M.; Patrini, M.; Miele, E.; Das, G.; Toma, A.; Zaccaria, R. P.; Di Fabrizio, E. 3d Hollow Nanostructures as

DOI: 10.1021/acsami.5b06887
ACS Appl. Mater. Interfaces 2015, 7, 23597−23604

Building Blocks for Multifunctional Plasmonics. *Nano Lett.* **2013**, *13* (8), 3553−3558.
(25) Ward, D. R.; Huser, F.; Pauly, F.; Cuevas, J. C.; Natelson, D. Optical Rectification and Field Enhancement in a Plasmonic Nanogap. *Nat. Nanotechnol.* **2010**, *5* (10), 732−6.
(26) Huang, Q.; Huang, Z.; Meng, G.; Fu, Y.; Lakowicz, J. R. Plasmonic Nanorod Arrays for Enhancement of Single-Molecule Detection. *Chem. Commun.* **2013**, *49* (100), 11743−5.
(27) Chou, S. Y.; Krauss, P. R.; Renstrom, P. J. Imprint of Sub-25 Nm Vias and Trenches in Polymers. *Appl. Phys. Lett.* **1995**, *67* (21), 3114.
(28) Kontio, J. M.; Simonen, J.; Tommila, J.; Pessa, M. Arrays of Metallic Nanocones Fabricated by Uv-Nanoimprint Lithography. *Microelectron. Eng.* **2010**, *87* (9), 1711−1715.
(29) Wu, W.; Hu, M.; Ou, F. S.; Li, Z.; Williams, R. S. Cones Fabricated by 3d Nanoimprint Lithography for Highly Sensitive Surface Enhanced Raman Spectroscopy. *Nanotechnology* **2010**, *21* (25), 255502.
(30) Kontio, J. M.; Husu, H.; Simonen, J.; Huttunen, M. j.; Tommila, J.; Pessa, M.; Kauranen, M. Nanoimprint Fabrication of Gold Nanocones with È10 Nm Tips for Enhanced Optical Interactions. *Opt. Lett.* **2009**, *34* (13), 1979−1981.
(31) Cottat, M.; Lidgi-Guigui, N.; Tijunelyte, I.; Barbillon, G.; Hamouda, F.; Gogol, P.; Aassime, A.; Lourtioz, J.-M.; Bartenlian, B.; de la Chapelle, M. L. Soft Uv Nanoimprint Lithography-Designed Highly Sensitive Substrates for Sers Detection. *Nanoscale Res. Lett.* **2014**, *9* (1), 623 (1−6)..
(32) Fleischer, M.; Weber-Bergioni, A.; Altoe, M. V.; Schwartzberg, A. M.; Schuck, P. K.; Cabrini, S.; Kern, D. P. Gold nanocone near-field scanning optical microscopy probes. *ACS Nano* **2011**, *5* (4), 2570−2579.
(33) Battista, E.; Causa, F.; Lettera, V.; Panzetta, V.; Guarnieri, D.; Fusco, S.; Gentile, F.; Netti, P. A. Ligand Engagement on Material Surfaces Is Discriminated by Cell Mechanosensoring. *Biomaterials* **2015**, *45*, 72−80.
(34) Harder, P.; Grunze, M.; Dahint, R.; Whitesides, G. M.; Laibinis, P. E. Molecular Conformation in Oligo(Ethylene Glycol)-Terminated Self-Assembled Monolayers on Gold and Silver Surfaces Determines Their Ability to Resist Protein Adsorption. *J. Phys. Chem. B* **1998**, *102*, 426−436.
(35) Khatayevich, D.; Gungormus, M.; Yazici, H.; So, C.; Cetinel, S.; Ma, H.; Jen, A.; Tamerler, C.; Sarikaya, M. Biofunctionalization of Materials for Implants Using Engineered Peptides. *Acta Biomater.* **2010**, *6* (12), 4634−41.
(36) Causa, F.; Della Moglie, R.; Iaccino, E.; Mimmi, S.; Marasco, D.; Scognamiglio, P. L.; Battista, E.; Palmieri, C.; Cosenza, C.; Sanguigno, L.; Quinto, I.; Scala, G.; Netti, P. A. Evolutionary Screening and Adsorption Behavior of Engineered M13 Bacteriophage and Derived Dodecapeptide for Selective Decoration of Gold Interfaces. *J. Colloid Interface Sci.* **2013**, *389* (1), 220−9.
(37) Cusano, A. M.; Causa, F.; Moglie, R. D.; Falco, N.; Scognamiglio, P. L.; Aliberti, A.; Vecchione, R.; Battista, E.; Marasco, D.; Savarese, M.; Raucci, U.; Rega, N.; Netti, P. A. Integration of Binding Peptide Selection and Multifunctional Particles as Tool-Box for Capture of Soluble Proteins in Serum. *J. R. Soc., Interface* **2014**, *11* (99), 20140718.
(38) Tabakman, S. M.; Lau, L.; Robinson, J. T.; Price, J.; Sherlock, S. P.; Wang, H.; Zhang, B.; Chen, Z.; Tangsombatvisit, S.; Jarrell, J. A.; Utz, P. J.; Dai, H. Plasmonic Substrates for Multiplexed Protein Microarrays with Femtomolar Sensitivity and Broad Dynamic Range. *Nat. Commun.* **2011**, *2*, 466.
(39) Corrigan, T. D.; Guo, S.; Phaneuf, R. J.; Szmacinski, H. Enhanced Fluorescence from Periodic Arrays of Silver Nanoparticles. *J. Fluoresc.* **2005**, *15* (5), 777−84.
(40) Hatab, N. A.; Hsueh, C. H.; Gaddis, A. L.; Retterer, S. T.; Li, J. H.; Eres, G.; Zhang, Z.; Gu, B. Free-Standing Optical Gold Bowtie Nanoantenna with Variable Gap Size for Enhanced Raman Spectroscopy. *Nano Lett.* **2010**, *10* (12), 4952−5.
(41) Indrasekara, A. S.; Meyers, S.; Shubeita, S.; Feldman, L. C.; Gustafsson, T.; Fabris, L. Gold Nanostar Substrates for Sers-Based Chemical Sensing in the Femtomolar Regime. *Nanoscale* **2014**, *6*, 8891.
(42) Vendrell, M.; Maiti, K. K.; Dhaliwal, K.; Chang, Y. T. Surface-Enhanced Raman Scattering in Cancer Detection and Imaging. *Trends Biotechnol.* **2013**, *31* (4), 249−57.
(43) Liu, H.; Zhang, L.; Lang, X.; Yamaguchi, Y.; Iwasaki, H.; Inouye, Y.; Xue, Q.; Chen, M. Single Molecule Detection from a Large-Scale Sers-Active Au(7)(9)Ag(2)(1) Substrate. *Sci. Rep.* **2011**, *1*, 112.
(44) Johnson, P. B.; Christy, R. W. Optical Constants of the Noble Metals. *Phys. Rev. B* **1972**, *6* (12), 4370−4379.
(45) Aspnes, D. E. the Accurate Determination of Optical Properties by Ellipsometry. In *Handbook of Optical Constants of Solids*;, Palik, E. D., Ed.; Academic Press: Boston, 1985; Chapter 5, pp 89−112.
(46) Viheriala, J.; Rytkonen, T.; Niemi, T.; Pessa, M. Narrow Linewidth Templates for Nanoimprint Lithography Utilizing Conformal Deposition. *Nanotechnology* **2008**, *19* (1), 015302.
(47) De Angelis, F.; Proietti Zaccaria, R.; Francardi, M.; Liberale, C.; Di Fabrizio, E. Multi-Scheme Approach for Efficient Surface Plasmon Polariton Generation in Metallic Conical Tips on Afm-Based Cantilevers. *Opt. Express* **2011**, *19* (22), 22268−22279.
(48) Proietti Zaccaria, R.; Alabastri, A.; De Angelis, F.; Das, G.; Liberale, C.; Toma, A.; Giugni, A.; Razzari, L.; Malerba, M.; Sun, H. B.; Di Fabrizio, E.. Fully Analytical Description of Adiabatic Compression in Dissipative Polaritonic Structures. *Phys. Rev. B: Condens. Matter Mater. Phys.* **2012**, *86* (3).03541010.1103/PhysRevB.86.035410
(49) Ray, K.; Lakowicz, J. R. Metal-Enhanced Fluorescence Lifetime Imaging and Spectroscopy on a Modified Sers Substrate. *J. Phys. Chem. C* **2013**, *117* (30), 15790−15797.
(50) Geddes, C. D. Metal-Enhanced Fluorescence. *Phys. Chem. Chem. Phys.* **2013**, *15* (45), 19537.
(51) Deng, W.; Xie, F.; Baltar, H. T.; Goldys, E. M. Metal-Enhanced Fluorescence in the Life Sciences: Here, Now and Beyond. *Phys. Chem. Chem. Phys.* **2013**, *15* (38), 15695−708.
(52) Song, J. H.; Atay, T.; Shi, S. F.; Urabe, H.; Nurmikko, A. V. Large Enhancement of Fluorescence Efficiency from Cdse/Zns Quantum Dots Induced by Resonant Coupling to Spatially Controlled Surface Plasmons. *Nano Lett.* **2005**, *5* (8), 1557−1561.
(53) Maiti, K. K.; Dinish, U. S.; Fu, C. Y.; Lee, J. J.; Soh, K. S.; Yun, S. W.; Bhuvaneswari, R.; Olivo, M.; Chang, Y. T. Development of Biocompatible Sers Nanotag with Increased Stability by Chemisorption of Reporter Molecule for in Vivo Cancer Detection. *Biosens. Bioelectron.* **2010**, *26* (2), 398−403.

DOI: 10.1021/acsami.5b06887
ACS Appl. Mater. Interfaces 2015, 7, 23597−23604